Simulation of Power Electronic Converters Using Quasi Steady State Approximation

Predrag Pejović

Faculty of Electrical Engineering
University of Belgrade
Belgrade, Serbia
peja@etf.rs

Abstract—**A new method to compute voltage and current waveforms of power electronic converters is proposed in the paper. The method relies on the simulation result of the averaged circuit model, and superimposes the ripple of the inductor currents to the obtained average values, assuming that the linear ripple approximation applies. To determine the amplitude of the switching ripple, a quasi steady state approximation is proposed. After the inductor currents are obtained, currents of switching components are computed by multiplying them with appropriate switching functions. The algorithm provides an efficient tool to generate the converter waveforms in order to compute their spectra, mean and RMS values, which are of interest in designing filters and estimating converter losses.**

Keywords-circuit averaging, linear ripple approximation, simulation, switched networks

I. INTRODUCTION

Circuit simulation in power electronics is a demanding task [1]. The simulation problems focus a variety of problems, ranging from the problems of switching transitions, characterized by short time intervals where the phenomena of interest occur, up to the long term simulations of pulse width modulated (PWM) line-connected converters, lasting for several periods of the line voltage, with the time span covering a huge number of switching transitions. In the later case, it is likely that the simulation output files would be huge, with the data points distributed in time in a nonuniform fashion. To make the things worse, it is possible that the simulation will not be completed due to the infamous "convergence problems". The convergence problems occur in Newton-Raphson iteration over nonlinearity [2], and they frequently follow simulations in power electronics since the essentially discontinuous waveforms encountered there cause the initial guess for the Newton-Raphson iteration to be poor in the vicinity of switching transitions. To overcome some of the problems mentioned, special simulation techniques intended for application on power electronic circuits have been developed [3, 4]. The methods are primarily based on piecewise linear device models, and avoid iteration over nonlinearity.

Increased use of switching converters result in increased concern about the electromagnetic interference (EMI). To design EMI filters [5], spectra of the converter currents are of interest. In the case of switching PWM converters connected to the line, in some cases there are analytical solutions for the spectra, expressed in terms of series involving the Bessel functions, according to the Jacobi-Anger expansion [6]. However, in most of the cases a numerical simulation approach is needed, which is a demanding task. The converter switching frequency is usually much higher than the line frequency, $f_S >> f_0$, thus simulation over many switching periods would be required. On the other hand, details of the switching transitions, in the case the switching is done properly, are not of particular interest in determining the converter current spectra. This is a motivation to develop a new simulation method that would neglect details of switching transitions and avoid infamous convergence problems, while providing the waveforms accurate enough to determine the spectra. A simulation method aimed in this direction is proposed in this paper. It is based on simulation of the converter averaged circuit model [7], while actual waveforms of the converter inductor currents are obtained by superimposing the switching ripple to the obtained averaged waveforms. To determine amplitude of the switching ripple, a newly introduced quasi steady state approximation is applied. In this manner, the waveforms are obtained in an efficient and reliable manner, avoiding the convergence problems.

To illustrate the simulation problems focused in this paper and to demonstrate the proposed algorithms, an inverter system shown in Fig. 1 is used as an example. The inverter system should supply an AC voltage source
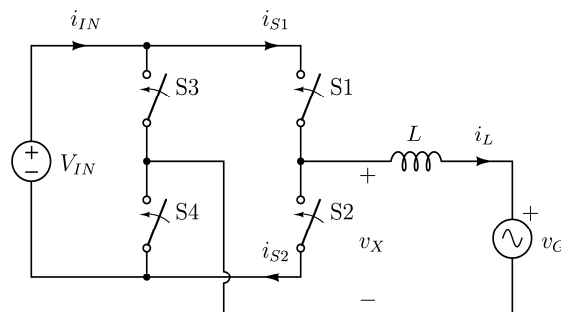
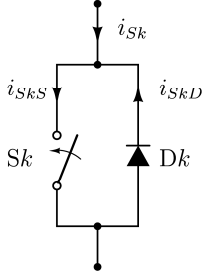$$v_G = V_m \cos(\omega_0 t) \qquad (1)$$

Figure 1.   The inverter system.

Figure 2.   The switch structure.

with the average current over the switching period

$$\overline{i_L} = I_m \cos(\omega_0 t). \tag{2}$$

In the examples analyzed in this paper, it is assumed that $V_m = 230\sqrt{2}$ V , $\omega_0 = 2\pi \times 50$ Hz , and that the current is programmed such that $I_m = 20$ A . To achieve this, the inverter is operated with the constant switching frequency of $f_S = 20$ kHz, with an appropriate duty ratio function $d(t)$, to be determined by the averaged circuit analysis. The input voltage is assumed constant, $V_{IN} = 450$ V , and the coupling inductor is assumed to have $L = 1.4$ mH . Each of the switches in the inverter is built using an unidirectional controlled switch and an antiparallel diode, as depicted in Fig. 2. The current of the switch i_{Sk} consists of the controlled switch current i_{SkS} and the diode current i_{SkD} according to

$$i_{Sk} = i_{SkS} - i_{SkD} . \tag{3}$$

The simulation problem is to determine the waveforms of i_L , i_{IN} aiming their spectra, as well as to determine the waveforms of i_{Sk} , i_{SkS} , and i_{SkD} for $k \in \{1,2,3,4\}$ aiming their average and RMS values to estimate the converter losses.

II.   THE AVERAGED CIRCUIT MODEL

The first step in obtaining the desired solution is to solve the averaged circuit. In the example focused in this paper, this step is going to be performed analytically and manually. However, solution of the averaged circuit can also be obtained numerically. This is not a difficult numerical problem, since the differential equations that characterize averaged circuits are smooth, because all of the averaged voltages and currents are continuous in time.

To inject the current i_L into the stiff voltage source v_G as specified by (2), the average of the inverter output voltage over the switching period should be

$$\overline{v_X} = v_G + L\frac{d\overline{i_L}}{dt} = V_m \cos(\omega_0 t) - \omega_0 L I_m \sin(\omega_0 t) . \tag{4}$$

This is achieved by the inverter switching with the duty ratio

$$d(t) = \frac{1}{2}\left(1 + \frac{v_X(t)}{V_{IN}}\right). \tag{5}$$

Waveforms of v_G , $\overline{v_L} = L\,d\overline{i_L}/dt$, and $\overline{v_X}$ are shown in Fig. 3, illustrating that the average voltage across the inductor is significantly lower than the surrounding voltages. This would be important for the approximations used in subsequent analyses.
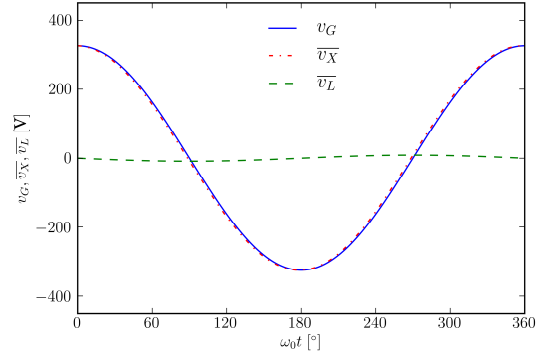

Figure 3.   Averaged voltages in the circuit.

III.   LINEAR RIPPLE APPROXIMATION

The first assumption required by the proposed method is that the linear ripple approximation applies. Focusing to a switching interval $0 < t < T_S$, $T_S = 1/f_S$, the linear ripple approximation assumes that the inductor voltage over the interval is a constant V_{L1} during $0 < t < dT_S$, and an another constant V_{L2} during $dT_S < t < T_S$. Under these assumptions, the inductor current ripple is a piecewise linear function of time. It will also be assumed that $V_{L1} > 0$ and $V_{L2} < 0$. The linear ripple approximation is used to analyze switching converters in steady state, where $i_L(T_S) = i_L(0)$. In that case, the amplitude of the inductor current ripple is given by

$$\Delta i_{L1} = \frac{V_{L1}}{2Lf_S} d . \tag{6}$$

or

$$\Delta i_{L2} = -\frac{V_{L2}}{2Lf_S} d' \tag{7}$$

which provides the same $\Delta i_L = \Delta i_{L1} = \Delta i_{L2}$ in the converter steady state operation, since according to the volt-second balance

$$V_{L1} d + V_{L2} d' = 0 . \tag{8}$$

IV. QUASI STEADY STATE APPROXIMATION

Purpose of the quasi steady state approximation is to determine envelope of the inductor current while the inductor is not in the steady state operation over the switching interval, i.e. $i_L(T_S) \neq i_L(0)$. Assuming that the inductor operation is not far from the steady state, amplitude of the inductor current ripple could be computed using (6) and (7). In the example circuit of Fig. 1, for the given set of parameters amplitudes of the inductor current ripple Δi_{L1} computed using (6) and Δi_{L2} computed using (7) are presented in Fig. 4. There is not a big difference between the waveforms, but still there is a difference. The difference could be computed as

$$\Delta\Delta i_L = \Delta i_{L1} - \Delta i_{L2} = \frac{V_{L1}d + V_{L2}d'}{2f_S L} = \frac{\overline{v_L}}{2f_S L} \qquad (9)$$

which fits to the waveform of the difference shown in Fig. 4. This indicates that having $\overline{v_L}$ low in comparison to the surrounding voltages is essential for application of the quasi steady state approximation, as already indicated.

To compromise between the two predictions of the inductor current ripple amplitude in the non steady state conditions, the average of the predictions is proposed, resulting in

$$\Delta i_L = \frac{V_{L1}d - V_{L2}d'}{4f_S L} . \qquad (10)$$

This formula for the inductor current ripple amplitude constitutes the quasi steady state approximation. In the case of the example circuit of Fig. 1, the formula provides the envelope of the inductor current as depicted in Fig. 5.

V. CONSTRUCTION OF THE CURRENT WAVEFORMS

The methods introduced this far are aimed to construct the waveforms of the converter currents. Essential waveform to be constructed is the waveform of the inductor current. The other waveforms are constructed applying the obtained inductor current waveform and appropriate switching functions.
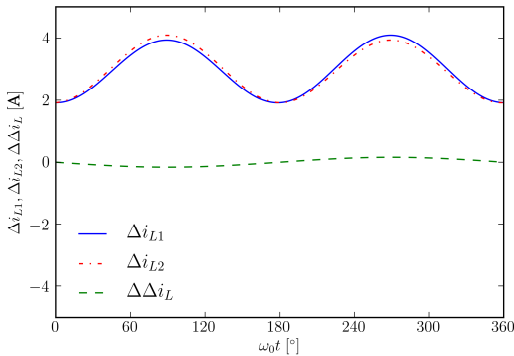
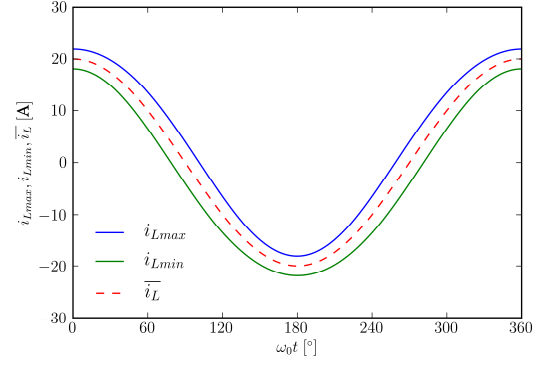Figure 4.   Amplitude of the inductor current ripple.
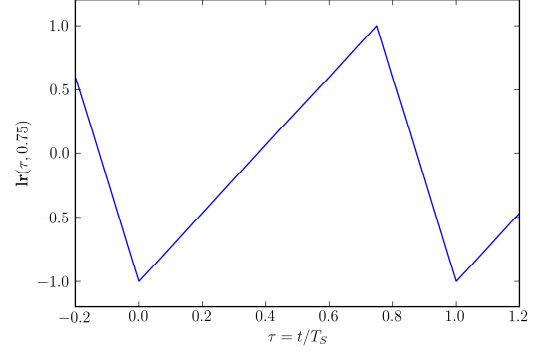
Figure 5.   Envelope of the inductor current.

Figure 6.   Definition of the $lr(\tau, d)$ switching function.

To construct the inductor current waveform, the switching ripple prototype function $lr(\tau, d)$ (lr stands for "linear ripple") depicted in Fig. 6 is applied, and the inductor current is obtained as

$$i_L(t) = \overline{i_L}(t) + \Delta i_L(t)\, lr(t, d(t)) \qquad (11)$$

where $\overline{i_L}(t)$ and $d(t)$ are obtained as a result of the averaged circuit analysis, while $\Delta i_L(t)$ is obtained applying the quasi steady state approximation proposed in this paper, in (10).

After the inductor current waveform is obtained, waveforms of the switch currents are constructed applying switching functions $d1(\tau, d)$ and $d0(\tau, d)$, defined in a similar manner as $lr(\tau, d)$, as depicted in Figs. 7 and 8. Application of the switching functions to construct the waveforms of i_{S1} and i_{S2} results in

$$i_{S1}(t) = i_L(t) \times d1(t, d(t)) \qquad (12)$$

and

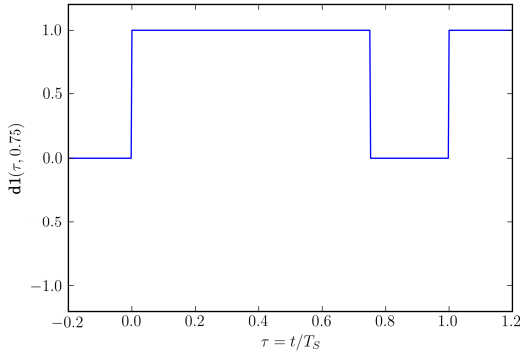$$i_{S2}(t) = i_L(t) \times d0(t, d(t)). \qquad (13)$$

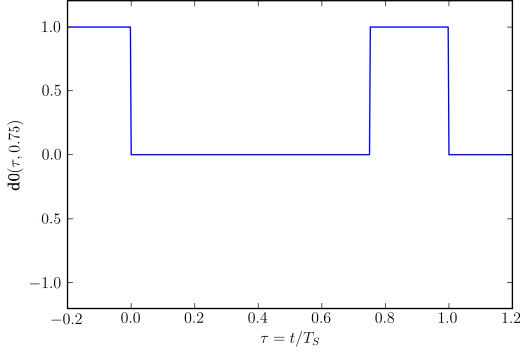Figure 7. Definition of the $\mathrm{d1}(\tau,d)$ switching function.

Figure 8. Definition of the $\mathrm{d0}(\tau,d)$ switching function.

It should be noted here that functions $\mathrm{d1}(\tau,d)$ and $\mathrm{d0}(\tau,d)$ take only values 0 or 1, which should be used to reduce the computational burden.

Functions $\mathrm{lr}(\tau,d)$, $\mathrm{d1}(\tau,d)$, $\mathrm{d0}(\tau,d)$ are introduced here in an intuitive fashion, by their diagrams for $d = 0.75$ shown in Figs. 6–8. Since the functions are piecewise linear, it is not a difficult task to obtain their analytical description, which is necessary for the software implementation, but avoided here due to the space limitations.

To separate the switch current to the controlled switch current and the antiparallel diode current, according to Fig. 2, the Heaviside function is applied to model the additional switching. The controlled switch current is obtained as

$$i_{S1S}(t) = i_{S1}(t) \times \mathrm{h}(i_{S1}(t)) \qquad (14)$$

while the diode current is obtained as

$$i_{S1D}(t) = -i_{S1}(t) \times \mathrm{h}(-i_{S1}(t)). \qquad (15)$$

The same technique is applied for the remaining switches of the inverter.

To determine the inverter input current, it is convenient to define an additional switching function, named d-selector function
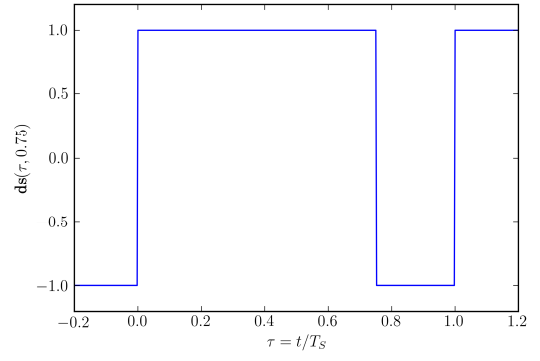

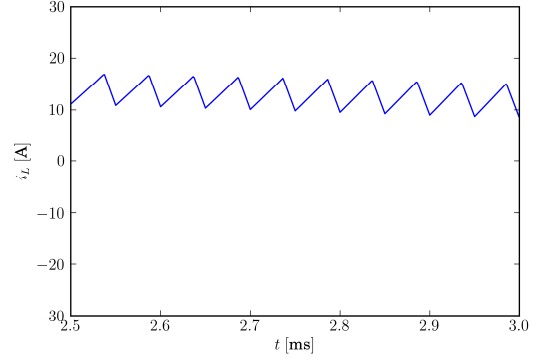Figure 9. Definition of the $\mathrm{ds}(\tau,d)$ switching function.

Figure 10. Simulation, constructed waveform of i_L.

$$\mathrm{ds}(\tau,d) = \mathrm{d1}(\tau,d) - \mathrm{d0}(\tau,d) \qquad (16)$$

shown in Fig. 9. This reduces construction of $i_{IN}(t)$ to

$$i_{IN}(t) = i_L(t) \times \mathrm{ds}(t, d(t)). \qquad (17)$$

VI. SIMULATION RESULTS

To illustrate the proposed algorithm and to fulfill the simulation requirements specified in the Introduction, the example circuit of Fig. 1 is simulated, i.e. waveforms of i_L, i_{IN}, i_{S1}, i_{S1S}, i_{S1D}, i_{S2}, i_{S2S}, and i_{S2D} are constructed, and their mean values, RMS values, and the spectra are determined. The first step in the simulation was to solve the averaged circuit, which is in this case done analytically, resulting in the waveforms of $\overline{i_L}$ (actually, this waveform has been initially prescribed), $\overline{v_X}$ and the duty-ratio function $d(t)$. The next step was to determine the amplitude of the inductor current ripple, which is done applying the quasi steady state approximation formalized by (10). Finally, the inductor current is constructed applying (11), which is followed by the construction of currents dependent on i_L: i_{IN}, i_{S1}, i_{S1S}, i_{S1D}, i_{S2}, i_{S2S}, and i_{S2D}. The waveforms obtained applying the described procedure are shown in Figs. 10–13 during ten switching
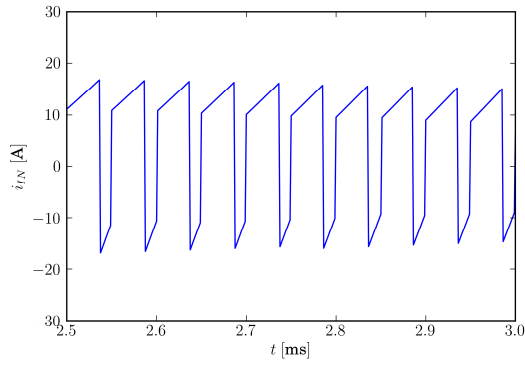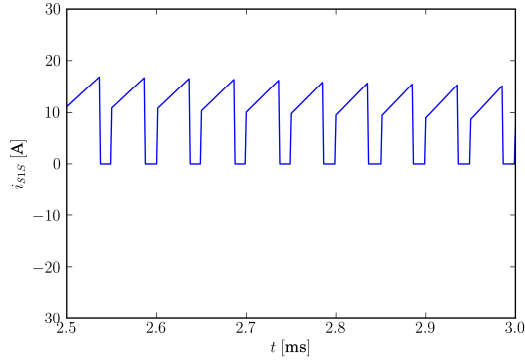
Figure 11. Simulation, constructed waveform of i_{IN}.

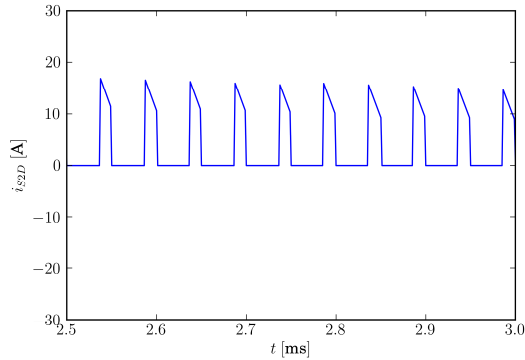Figure 12. Simulation, constructed waveform of i_{S1}.

Figure 13. Simulation, constructed waveform of i_{S2}.

intervals in the time segment from 2.5 ms to 3 ms. The waveforms are in agreement with the theoretical expectations. Significant ripple in the waveform of i_{IN} is observed, indicating a strong need for its filtering.

After the waveforms are obtained in 16000 regularly placed samples over the line period, using the Discrete Fourier Transform (DFT) and slight post-processing the one-sided spectra of i_L and i_{IN} are obtained as presented in Figs. 14 and 15. The spectra are shown with the frequency axes normalized to the switching frequency f_S, to illustrate that the spectral components group at the multiples of f_S.
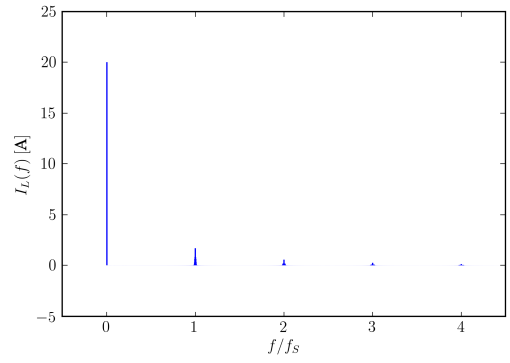

Figure 14. Simulation, spectrum of i_L.
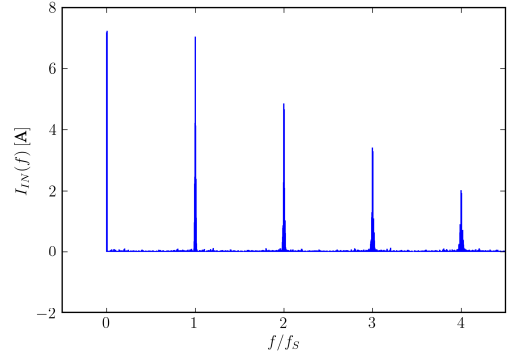

Figure 15. Simulation, spectrum of i_{IN}.

In Fig. 14, a fundamental harmonic component at f_0 with the amplitude of 20 A can be observed, which meets the initial requirements. The DC component of i_L is equal to zero. On the other hand, the DC component of i_{IN}, $I_{IN} = 7.20$ A, matches the value predicted applying the conservation of energy. Dominant AC component in i_{IN} spectrum at low frequencies is at $2f_0$, with the amplitude of 7.25 A, which also meets the theoretical predictions obtained analyzing the averaged circuit. These two components could hardly be distinguished in the diagram of Fig. 15, since they are close one to another, and to observe them separately requires rescaling of the diagram.

By post processing of the constructed waveforms, the RMS value of i_{IN} is obtained, being equal to $I_{IN,RMS} = 14.25$ A. The value this high is caused by the significant content of the higher order harmonics. On the other hand, the RMS value of i_L, $I_{L,RMS} = 14.25$ A is negligibly higher than the RMS value of its first harmonic of 14.14 A. Comparing the spectra of Figs. 14 and 15, it can be concluded that i_{IN} is significantly more polluted with the higher order harmonics than the waveform of i_L.

Finally, the average and the RMS values of i_{S1S}, i_{S1D}, i_{S2}, i_{S2S}, and i_{S2D} are obtained as $I_{S1S} = 5.05$ A, $I_{S1D} = 1.45$ A, $I_{S2S} = 4.96$ A, $I_{S2D} = 1.36$ A, while $I_{S1S,RMS} = 9.07$ A, $I_{S1D RMS} = 4.56$ A, $I_{S2S RMS} = 8.99$ A, $I_{S2D RMS} = 4.38$ A. This

enables computation of losses in the switching elements, and concludes the circuit analysis according to the initially stated requirements.

The simulation results are obtained by a program written in Python programming language [8], in PyLab environment, relying entirely on free software tools. The PyLab environment is chosen since it provides a comfortable access to NumPy and SciPy packages, that were used to provide array type objects and to perform numerical computations, like the Discrete Fourier Transform. Besides that, the PyLab environment provides a comfortable access to matplotlib package, which was used to plot the graphs shown in Figs. 3–15. The numerical simulation without generating the plots was completed in 2.09 s on a PC computer equipped with Intel Q8200 processor run at 2.33 GHz under Ubuntu 12.04 operating system. However, to perform the simulation, to generate the plots with LaTeX lettering, and to store them with 600 dpi resolution, took 19 s, indicating that the most of the runtime is spent on generating the graphs. Comparison to conventional simulation tools, like SPICE derivatives, naturally arises. However, it is not possible to perform a fair comparison, since the proposed simulation algorithm does not provide information about details of switching transitions, which generates the most of the computational burden in the conventional tools. Overall impression is that the simulation is much faster and much easier to perform, void of convergence problems, but the simulation result is different in the level of details provided. On the other hand, details of switching transitions provided by the conventional simulation tools rely on accurate component models that are not always available, which questions validity and meaning of the detailed simulation.

VII. CONCLUSIONS

In this paper, a novel method for simulation of switching power converters is proposed. The method is aimed to determine spectra of the converter currents and their mean and RMS values in cases where details of switching transitions are not of interest. Waveforms of the converter currents are constructed starting from the average currents of the inductors, superimposing the ripple waveforms to the average values in order to obtain the instantaneous value waveforms. Validity of the linear ripple approximation is assumed. To compute the ripple amplitude, a newly introduced quasi steady state approximation is used. Waveforms of the currents of the switching components are treated as dependent, and obtained from the currents of the inductors applying appropriate switching functions. The resulting algorithm is numerically efficient and void of the convergence problems. The output waveforms are obtained in the form of regularly sampled signals, suitable for the Fourier analysis. The method is initially meant to be applied in the EMI filter design.

Work in progress regarding the algorithm includes:

1. Further formalization of the algorithm, primarily in the area of the averaged circuit analysis.

2. Quantitative analysis of the error introduced by accepted approximations.

3. Generalization of the method to include converters operating in the discontinuous conduction mode.

4. Quantitative characterization of the error introduced by the choice of DFT parameters, primarily the number of harmonics computed (related to the number of samples taken) and the spectral resolution (related to the number of line periods taken in the analysis).

5. Experimental confirmation of the results.

REFERENCES

[1] D. Maksimović, A. M. Stanković, V. J. Thottuvelil, G. C. Verghese, "Modeling and simulation of power electronic converters," *Proceedings of the IEEE*, vol. 89, no. 6, pp. 898–912, June 2001.

[2] A. Vladimirescu, The SPICE Book, John Wiley, 1994.

[3] P. Pejović, D. Maksimović, "A new algorithm for simulation of power electronic systems using piecewise-linear device models," *IEEE Transactions on Power Electronics*, vol. 10, no. 3, pp. 340–348, May 1995.

[4] D. Li, R. Tymerski, and T. Ninomiya, "PECS—An efficient solution for simulating switched networks with nonlinear elements," *IEEE Transactions on Industrial Electronics*, vol. 48, no. 2, pp. 367–376, April 2001.

[5] R. W. Erickson, D. Maksimović, *Fundamentals of Power Electronics*, 2nd ed. Norwell, MA: Kluwer Academic, 2001.

[6] B. P. McGrath, D. G. Holmes, "An Analytical Technique for the Determination of Spectral Components of Multilevel Carrier-Based PWM Methods," *IEEE Transactions on Industrial Electronics*, vol. 49, no. 4, pp. 847–857, August 2002.

[7] A. Davoudi, J. Jatskevich, T. De Rybel, "Numerical state-space average-value modeling of PWM DC-DC converters operating in DCM and CCM," *IEEE Transactions on Power Electronics*, vol. 21, no. 4., pp. 1003–1012, July 2006.

[8] H. P. Langtangen, *A Primer on Scientific Programming with Python*, Berlin: Springer, 2009.